Electronic Population on Tungsten, Molybdenum, and Vanadium Atoms and ^{183}W, ^{95}Mo, and ^{51}V NMR in Polyoxometalates

Leonid P. Kazansky*

Institute of Physical Chemistry, Russian Academy of Sciences, 31 Leninski pr. 117071 Moscow, Russia

Toshihiro Yamase

Research Laboratory of Resources Utilization, Tokyo Institute of Technology, 4259 Nagatsuta, Midori-ku, Yokohama 227, Japan

Received: March 31, 2004; In Final Form: May 25, 2004

For a large number (more than 60) of polyoxometalates (POM) of tungsten, molybdenum, and vanadium, the charges on metal cations of the coordination sphere have been calculated using the extended Hückel molecular orbital method, and obtained values are compared with the NMR chemical shifts of the corresponding nuclei. Depending on the local geometry around the metal cation formed by oxygen atoms that may be different in the large POM, the ^{183}W NMR chemical shifts (for tungstates in the range of +268 ppm to −300 ppm or even larger, if the shift of −670 ppm for phosphoperoxotungstate is taken into account) correlate with the charges created by the oxygen environment (q in a range from 3.893 to 3.521 and 3.280 for phosphoperoxotungstate). It was assumed that the charge created on the metal cation reflects the change in the energy of the virtual molecular orbitals participating in the magnetically dipole-allowed transitions affecting the paramagnetic contribution that is the determining term in the variation of the chemical shift. As a general rule, decreasing positive charge (increased electronic population) on the metal cation results in decreased chemical shift, i.e., corresponding to its *shielding*. Similar conclusions are made concerning the ^{95}Mo and ^{51}V NMR chemical shifts, if they are compared with the calculated charges for the corresponding nuclei. It was shown that some deviations from the observed tendency are often due to the fact that some bond lengths in the X-ray structure determination are out from their usual range. If allowance is made for the usual range of the bond lengths (mainly in the bond with the terminal oxygen atom) the observed trend "chemical shift/charge" is conserved. This situation should be distinguished from the case of the *reduced diamagnetic* POM, where an increase in the electronic population on the given atom results in its *deshielding* due to the increased paramagnetic electron circulation. Roughly, the ^{183}W NMR chemical shifts (in a range from +60 to +1500 ppm) linearly depend on the excess of the charge acquired by the given atom upon reduction. Calculations also show which atoms participate in LUMO of POM and consequently which cations are reduced. Such conclusions are consistent with observed chemical shifts of the reduced forms of POM.

1. Introduction

A large number of polyoxometalates (POM) are formed by tungsten, molybdenum, and vanadium in the highest valence states.[1−4] In most cases, the anionic structures use octahedral building blocks WO_6, which can be linked by edges and/or corners forming, sometimes, unusual architecture both in solids and solutions. Because of versatile properties, they find many various applications. Many spectroscopic methods are used to study them, and one of them is multi-NMR. Nuclear shielding provides a tool for understanding the electronic and molecular environments of a nucleus. In studying NMR spectra of different nuclei in a given anion, one gets a unique possibility to elucidate electronic distribution and structure of a POM in great detail.[4,5]

Among many nuclei, the ^{183}W and ^{51}V NMR are most popular and the chemical shift reflects the electronic environment of an atom under study, because in many cases, the nonequivalent surrounding induces different chemical shifts. However, there is no direct demonstration of the bonding in the value of the chemical shift like it can be seen, for example, in vibration spectroscopy. For polyoxotungstates of W(VI), the span of the chemical shifts may spread from 260 to −300 ppm and even up to −670 ppm, if the peroxocomplexes are taken into account. Unpaired electrons in paramagnetic complexes or paired electrons (electrons in metal−metal bonds or a delocalized electron pair) in reduced species may induce the chemical shifts from +2500 to −4000 ppm. (See references in refs 5 and 6.) The possibility to observe the NMR signals for POM in the solid state opens new perspectives in studying the molecular and electronic structures of such molecules and in understanding their role in many processes.

The first attempt to explain a trend in the change of the ^{183}W NMR chemical shift was probably given by Gansow et al.[7] by the charge delocalization resulting from a removal of one W=O group from the Keggin anion $PW_{12}O_{40}^{3-}$ with formation of a lacunary anion $PW_{11}O_{39}^{7-}$. On this basis, the assignment of observed lines to the distinct tungsten atoms in the structure was made. However, later this assignment was proved to be wrong, and the actual attribution was made using difference in the spin−spin coupling $^2J_{W-O-W}$ observed around the main lines.[8] The connectivities between different tungsten atoms

* To whom correspondence may be addressed. E-mail: leoka@ipc.rssi.ru.

10.1021/jp0485993 CCC: $27.50
Published on Web 07/02/2004

obtained by two-dimensional ^{183}W NMR have been used for an unequivocal assignment of the lines to tungsten atoms in the structure. However, such coupling is actually observed only in the favorable cases, when a good signal-to-noise ratio is achieved.

The assignment of the lines is certainly easy when the number of nonequivalent atoms is different, giving rise to different intensities of the observed lines, or in some cases, it can be inferred from the width of the lines.[9] It is found that, because of the extreme sensitivity of ^{183}W shielding, the chemical shift depends on even minor environmental changes. For some POMs, the ^{183}W NMR chemical shifts correlate with the mean bond length in individual octahedra,[10] similar to correlations found by Mason[11] between the increasing shielding (more negative NMR chemical shifts) and compression of polyhedron around the nucleus under study.

As known, the chemical shift is determined by two principal terms: diamagnetic and paramagnetic.[6] The diamagnetic contribution σ_d is due to the field induced by electron circulation within an atom in an applied external magnetic field. The paramagnetic term σ_p arises from the mixing of the excited states (magnetic dipole allowed) with the ground electronic state in the presence of the applied magnetic field. Usually, and as calculations show, the diamagnetic contribution does not vary within a series of similar complexes.[6] The paramagnetic term depends on the summation of the inverse energy separations between the occupied and virtual MO and the less energy transition, the larger chemical shift should be observed.

The principal contribution of the paramagnetic term in a change of the chemical shift was shown by linear correlation between the ^{183}W NMR chemical shift and the wavelength of the lowest charge transfer (LCT) band for the Keggin $XW_{12}O_{40}^{n-}$ anions depending on X, despite the fact that this transition is not magnetically dipole allowed.[12] However, such a correlation can be found only for closely related complexes, because the lowest-unoccupied molecular orbital(s) (LUMO) participates also in magnetically dipole-allowed transitions.[6]

Taking into account dependence of the chemical shielding on $1/\Delta E$, an extended Hückel molecular orbital method (EHMO) calculation was used to find the energy difference between bonding and antibonding MOs for the isolated polyhedron taken out the POM framework (averaged structure in the adopted general symmetry of POM) and to follow the change in the ^{183}W NMR chemical shifts.[13] Thus, the paramagnetic contribution was shown to be a major factor in the change of the chemical shift in such molecules.

Difficulties arise when an isolated fragment is used, because it is unclear how differences in the bridging oxygen atoms (corner and edge sharing with different angles W−O−W) should be taken into account. Therefore, any calculations accounting the whole structure are highly desirable. However, increasing the number of atoms in molecules results in a large set of the molecular orbitals that may be involved in the electronic transitions, and they should be taken into account for calculation. There are several papers concerning calculation of the chemical shielding for ^{95}Mo, ^{51}V, and ^{183}W by different methods both ab initio and DFT.[14−19] Despite using sophisticated methods, discrepancies between the calculated and observed chemical shifts are rather large, even for small and simple mononuclear molecules, and ligands are too different allowing notable change in the chemical shift (more than 400 ppm), if one ligand is replaced by other. The first attempts to calculate the ^{183}W NMR chemical shifts in $PW_{12}O_{40}^{3-}$[20] and lacunary anions[21] by DFT were not so successful for deducing any conclusion on the reasons that change the chemical shift. Moreover, it seems that the optimization of a structure, especially when mixed addenda POM are considered, may result in opposite trends in the chemical shifts,[21] because sometimes even slight modification of the bond lengths (much less than obtained in the optimization) results in larger change of the chemical shift. As it was shown in ab initio calculations of the magnetic shielding of the ^{95}Mo nucleus in simple tetrahedral complexes, shortening the bond lengths Mo−O in MoO_4^{2-} by 0.022 Å results in a 317 ppm increase of the calculated Mo chemical shielding.[14] Such a compression of the tetrahedron gives better interaction of the atomic orbitals of metal and oxygen, resulting in larger energy separations and, hence, in less paramagnetic shift. At the same time, a more compact configuration builds up more electron density on metallic cation decreasing the positive charge and it goes parallel to the increasing energy separations.

Dependence of the nucleus shielding on the electronegativity of the neighbors is known, and the shielding correlates with a decrease in atomic electron density.[6] For example, there are numerous studies showing the trends of the chemical shifts with the calculated charges on the given nucleus.[6,14,20−23] In some cases a linear correlation between the chemical shifts and the calculated charges has been observed, especially for simple complexes, when one-ligand atoms, for example, O^{2-}, are gradually replaced by others, such as in simple complexes $[MoO_{4-x}S_x^{2-}]$.[14] (See Supporting Information, Figure S1 and Table S1 with DFT- and EHMO-calculated charges for $WO_{4-x}S_x^{2-}$ and other complexes). However, in such cases, the opposite trend is observed, namely, decreasing the positive charge on metal correlates with the deshielding. But we should bear in mind that the decreasing ΔE may affect much larger than the effect of the increased electron population on a nucleus.

In the large POM, the ligand atoms are the oxygen atoms, and only the type of oxygen (bridging or terminal) may affect the electronic distribution around the metal of the coordination sphere, and therefore, it would be interesting to see whether the ^{183}W and other nuclei NMR chemical shifts correlate with the electron population on metallic atoms of the coordination sphere with the aim to find a general trend, if the whole anion is used in calculation, and to use calculated values for assigning the observed NMR lines to the particular nuclei forming POM. It is the first objective for calculating the charges that are built up on the metal atom depending on the site environment. The second aim is to determine the distribution of the electron density, when two or more electrons are introduced upon reduction into the coordination sphere, and influence of the electron density on the NMR chemical shifts in this case. And the third one, as it proved after our analysis, results in the possibility to make some conclusions on the accuracy of the crystal structure determination. Actually, in most cases, according to the X-ray crystal data, despite assumed high symmetry of an anion, the environment around tungsten atoms, even for the similar local symmetry, is different due to some inaccuracy in the determination of the atomic coordinates and the influence of the crystal packing. Therefore for calculating the electronic structure of the whole anion, all symmetry-equivalent bond lengths are averaged under constraints of the expected symmetry of a whole anion. However, this approach is rather time consuming. In the present work for calculating the charges on metallic atoms, we follow a simple way using the crystallographic atomic coordinates and then the calculated charges are averaged for a particular type of metallic atom in a structure. The averaged charges and the charges obtained after calculation on the average structure may differ sometimes by 0.03 units.

However, if there are two or three different types of atoms in the anionic structure, we get the similar trends in the change of the charges for the averaged anion with an adopted high symmetry and the averaged charges for the same anion having symmetry, generally not higher than C_1.

Despite the simplest of the all valence one-electron theories, the EHMO approach provides a rather good and obvious initial approximation to the electronic structure of large and complex anions, sometimes with low symmetry.[24] We should also mention that, though the charges on metallic atoms may differ depending on the method used, there is parallel change of the calculated charges (for example, calculated by DFT) on metallic cation in some considered complex anions.

Another point should be also mentioned. For a heavy nucleus such as ^{95}Mo and especially ^{183}W, large relativistic and spin−orbital contributions into the shielding are expected.[6,17,18] However, for the polyoxotungstates, where tungsten is surrounded often by the same number of oxygen atoms, the difference in these contributions may be assumed to be small. The same may be said about the diamagnetic contribution that will be relatively constant throughout the whole series and therefore only variation in the paramagnetic contribution will play a principal role in the change of the chemical shift.

3. Results and Discussion

In all cases, experimental ^{183}W and ^{95}Mo NMR chemical shifts are referenced to one of $Na_2W(Mo)O_4$. For ^{51}V, the chemical shifts are recalculated relative to VO_4^{3-} (equal to −536 ppm, if referred to common standard $VOCl_3$). Along with this, we should mention that depending on the solvent the chemical shift may differ and usually in aprotic solvent the observed lines are shifted to high frequencies (more positive) (up to 20−30 ppm).

To calculate the charges on cations in polyoxometalates, the EHMO method of the HYPER6 package is used with minimal basis set of valence Slater orbitals and the Hückel parameter is set to 1.75. Input parameters for EHMO calculations are given in Table S2 in Supporting Information. In all cases, the experimental atomic coordinates taken from the X-ray crystal data (usually given as a CIF file) have been used. In cases when for the same polyanion there were several published data, the averaged calculated charges are given.

^{183}W NMR Chemical Shifts. Almost all studied anions may be regarded as derivatives of the two highly symmetrical structures: the compact Lindqvist anion $W_6O_{19}^{2-}$ (**I**) (Figure 1), where each WO_6 has a terminal oxygen atom and four edge-sharing bridging oxygen atoms,[25,26] and the Keggin anion[27] $[\alpha\text{-}XW_{12}O_{40}]^{3-}$ (α-**II**) (Figure 2), where four edge-shared triplet W_3O_{13} groups linking by corners form an inner tetrahedron occupied by heteroatom X. Twelve octahedra are equivalent, and each has one terminal bond, two corner-shared and two edge-shared oxygen atoms and one common to three tungstens and central atom. The local symmetry of each octahedron in both cases may be considered as C_{4v}.

Six equivalent tungsten cations in the original anion $W_6O_{19}^{2-}$ reveal the large chemical shift (Table 1). Removal of the W═O group results in the nonequivalency of tungsten atoms, one apical (W_A) and four belt (W_B) types (Figure 1). The derivative anion $W_{10}O_{32}^{4-}$ (**Ia**),[28,29] that may be viewed as two fused penta fragments of the parent anion, gives rise to the expected two-line pattern in the ^{183}W NMR spectrum shifted to lower values despite the lower energy of the lowest charge transfer (LCT) band (namely, excitations from MO formed mostly by oxygen orbitals to MO formed by tungsten ones), which should, in principle, lead to higher deshielding.[30,31] Hence, this transition does not contribute to the observed chemicals shifts. The line assigned to the apical tungsten atoms (W_A) is the most shifted. At the same time, the calculated charges on both types of tungsten atoms are less than those for the parent anion, and for

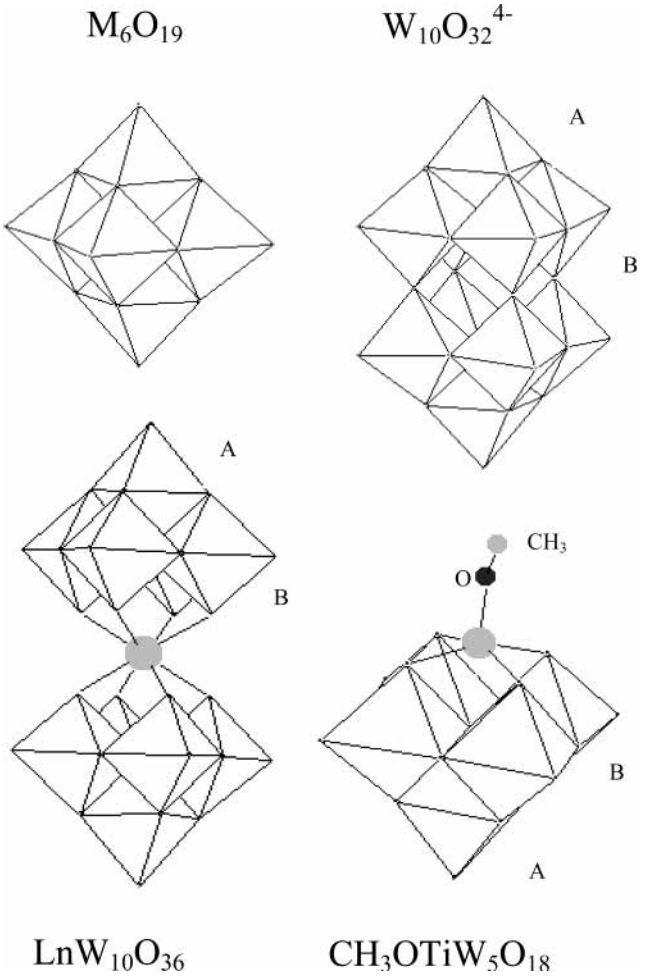

Figure 1. Structure of the Lindqvist anion and its derivatives.

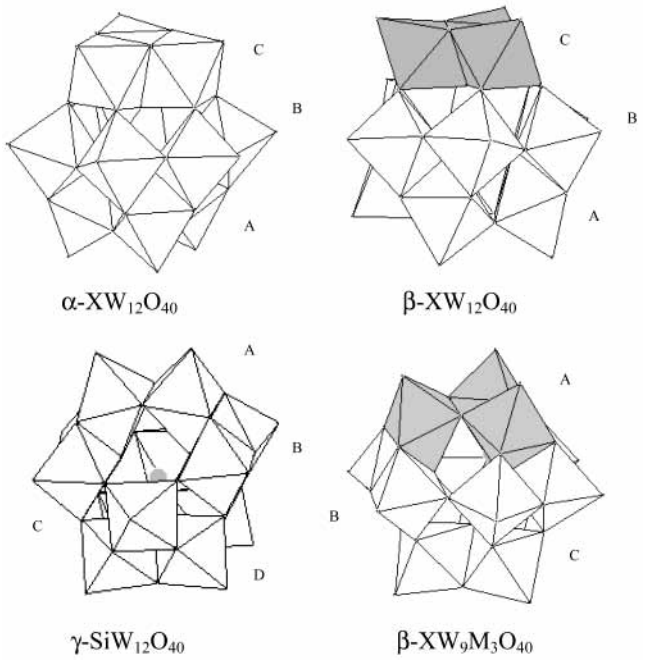

Figure 2. The structure of the Keggin anion and its isomeric forms.

TABLE 1: ^{183}W Chemical Shifts and Calculated Charge on Tungsten Atom in Polyoxotungstates

	POM	type		W_A	W_B	ref
1	$W_6O_{19}^{2-}$	I	q	3.737 (3.756)[a]		25, 26
			δ	59		7
2	$W_{10}O_{32}^{4-}$ [b]	**Ia**	q	3.659	3.736	28, 29
			δ	−160	−25	30, 31
3	$CeW_{10}O_{36}^{8-}$	**Ib**	q	3.749	3.731	33
			δ	−12	−17	35
4	$LaW_{10}O_{36}^{9-}$	**Ib**	q	3.709	3.716	34
			δ	−19	2	35
5	$CH_3TiW_5O_{19}^{3-}$	**Ic**	q	3.744	3.733	36
			δ	64.5	32.3	

[a] Value calculated for averaged bonds in the anion of O_h symmetry. [b] Average values calculated for structural data of two different papers.

the apical tungsten, the charge is the least one (Table 1). The same distribution of charges has been revealed by DFT calculations.[32] Thus, changing the structure (formation of the corner sharing W_B-O-W_B bonds) results in decreasing the charges on tungsten atoms.

From consideration of the structure, it is clear that practically linear bridges by oxygen atoms in the mirror plane induce lengthening in the W_B-O_{ab} bond in trans position and, consequently, the bonds W_A-O_{ab} are shortened, resulting in a decrease in the charge on W_A. Thus, an increase in the electronic population (decreased positive charge) results (as we will see below) in expected shielding of the corresponding nucleus. For this anion, we should note that the line for the apical tungstens, which have only edge-sharing oxygen atoms in the *xy* plane (perpendicular to the terminal W═O bond), reveals unusual high shielding. It should be mentioned that for the averaged structure we have a larger difference in the calculated charges. Nevertheless, the correspondence between the chemical shifts and the calculated charges is observed.

In $[LnW_{10}O_{36}]^{n-}$ (**Ib**), two penta fragments are coordinated by Ln cations (Figure 1).[33,34] In this anion, also two types of tungsten atoms and in cases of the diamagnetic complexes (La(III) and Ce(IV)) a two-line pattern is observed,[35] but the difference between δ is much less than for decatungstate $[W_{10}O_{32}]^{4-}$. The crystal structure determination has not been done for $[LaW_{10}O_{36}]^{9-}$, and for comparison, the charges are calculated using the structural parameters taken from the crystal structure determination of the Pr(III) complex.[34] Pr(III) should not induce many differences in the structural characteristics because of a similar lanthanide ionic radius. It should be noted that the calculated charges for the apical W_A, whose environment is apparently similar in the La and Ce complexes, also explains the reversed pattern[35] of two lines in the ^{183}W NMR spectrum of $[Ce(IV)W_{10}O_{36}]^{8-}$. It seems that the slightly larger W_A═O distance in the latter compared with $LaW_{10}O_{36}^{9-}$ results in a larger charge on W_A.

In some cases, the Lindqvist anion $[W_6O_{19}]^{2-}$ may give derivatives, where one or two groups W═O are replaced with other metal cation(s). Generally for monosubstituted anions, two lines with the intensity ratio 4:1 (the first number corresponds to the line with the highest chemical shifts) are observed (Table S3 in Supporting Information), but for $[(CH_3)OTiW_5O_{18}]^{3-}$, whose structure has been solved (Figure 1), the pattern in the ^{183}W NMR spectrum is reversed (Table 1)[36] and such change may be explained by the trans influence of Ti through the bridging oxygen atoms.[37,38] The calculated charges correspond to the observed chemical shifts. Some possible variations of the charges on metallic cations in some determined structures but without NMR data and vice versa are given in Table S3 (Supporting Information).

TABLE 2: ^{183}W Chemical Shifts and Calculated Charges in Isomeric Forms of the Keggin Anion and Its Isomeric and Mixed Species

	POM	charge shift, ppm	W_A	W_B	ref
6	$PW_{12}O_{40}^{3-}$	q	3.656		27
		δ	−93		12
7	B-β-$PW_9V_3O_{40}^{6-}$	q	3.680	3.650	41
		δ	−107	−118	42
	B-α-$PW_9V_3O_{40}^{6-}$	q	3.655	3.692	
	reconstructed	δ	−130	−87	43
8	B-β-$SiW_9Nb_3O_{40}^{7-}$	q	3.674	3.696	44
		δ	−125	−118	
9	B-β-$PW_9(NbO_2)_3O_{37}^{6-}$	q	3.697	3.701	45
		δ	−109	−111	

A number of POMs may be considered as derivatives of the Keggin anion (α-**II**) (Figure 2), from which the corner-shared triad group A or edge-shared triplet group C may be removed to give the ratio 3:6 (or 6:3) of tungsten atoms.

In some cases, the triad A may be replaced by a triad of other metal cations such as V(V), Nb(V), Ti(IV), and others (Figure 2, shaded octahedra). In many cases, the replacement of two and more tungsten atoms gives rise to so-called positional isomers,[39,40] and special preparative methods were developed to produce isomers with the predetermined disposition of introduced cations. However, because of the positional disorientation in the crystal, it is impossible to get geometric characteristics of the distinct isomer form the X-ray structure determination. Nevertheless, in some cases, authors have succeeded to prepare a crystal with the fixed orientation of anions.

For example, in the mixed addenda anion β-$XW_9M_3O_{40}^{6-}$ (Figure 2), three vanadium atoms replace the tungsten atoms in the triad (W_A).[41] But in this case, the triplet cap C is rotated around a 3-fold axis for 60°. In this mixed anion, the charge on the tungsten in the rotated triplet (W_C) is higher than one on tungsten in the belt B and the NMR chemical shift is also larger, coinciding with the observed trend in the charges and chemical shifts (Table 2).[42] It is noteworthy that calculation using a modeled $[\alpha\text{-}PW_9V_3O_{40}]^{6-}$, where triad A ($W_3O_6$) of the $[\alpha\text{-}PW_{12}O_{40}]^{3-}$ is replaced by V_3O_6 with coordinates taken from β-$PW_9V_3O_{40}^{6-}$, results in a larger charge on the belt tungsten than on the triplet ones, and therefore it may explain the inverse pattern of the lines in the ^{183}W spectrum of the α-mixed addenda anion (in italics in Table 2).[43]

For $[\beta\text{-}SiW_9Nb_3O_{40}]^{7-}$, whose structure was determined by Nomya et al.[44] similar to the phosphovanadotungstate one, the calculated charges on tungsten atoms in the triplet are less than in the six W belt, which is consistent with the observed two-line pattern in the ^{183}W NMR spectrum.

Another case of the substituted POM is peroxo complex $[\beta\text{-}PW_9(NbO_2)_3O_{37}]^{6-}$, where the terminal oxygen atoms on Nb (in triad A) are replaced by peroxo groups.[45] Both the calculated charges and the observed ^{183}W NMR chemical shifts for the cap W_C and belt W_B tungsten atoms are found to be very close, which rules out the possibility to discriminate the tungsten atoms and possibly subtle change in the electronic structure results in hardly distinguishable two lines.

The surface oxygen atoms O_e (edge type) or O_c (corner type) of the Keggin fragment XW_9O_{33} may be united giving in the former case so-called Dawson anions $[P(As)_2W_{18}O_{62}]^{6-}$ (**III**) (Figure 3).[46,47] Despite lowering the energy of the LCT band in comparison with the parent Keggin anion, the two lines with a 1:2 pattern intensity are shifted to negative values (Table 3).[48] Once again, we can underline that the LCT does not play an

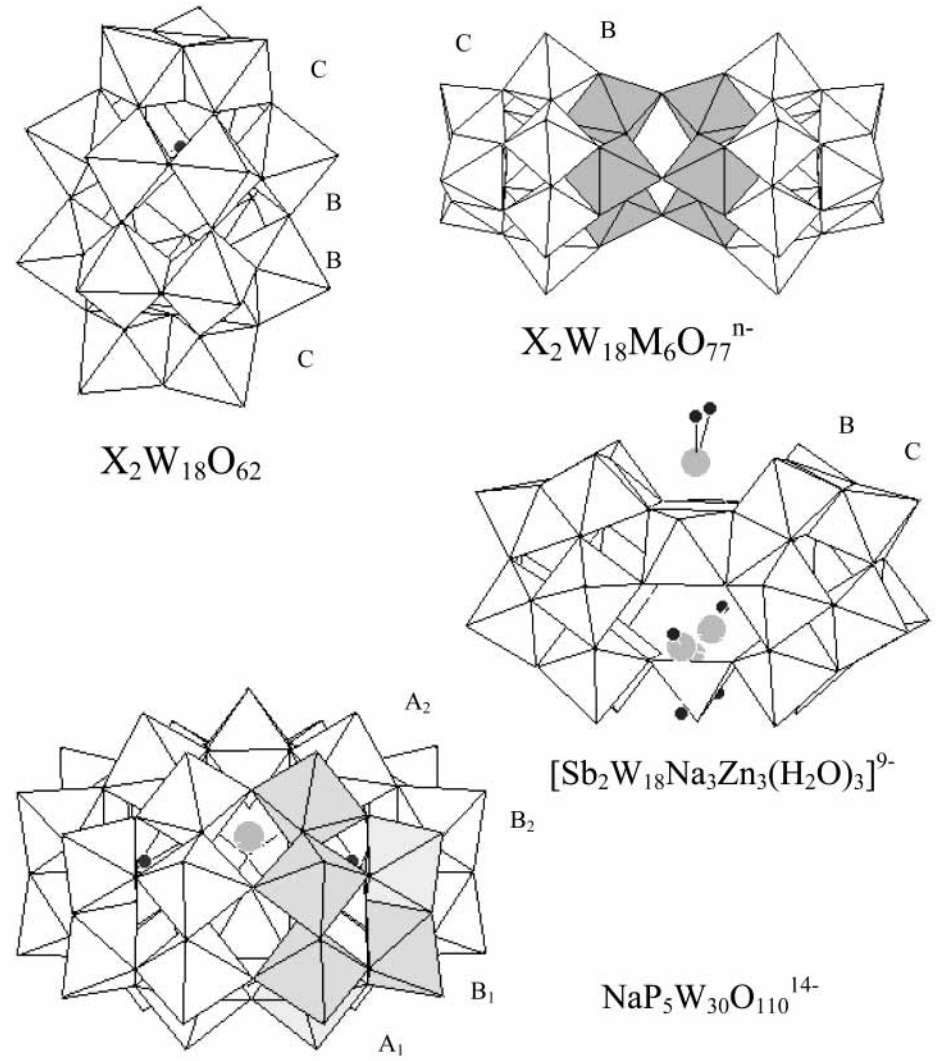

Figure 3. Structures of dimeric anions and $NaP_5W_{30}O_{110}^{14-}$ based on the Keggin anion fragments.

TABLE 3: ^{183}W Chemical Shifts and Calculated Charge in Complex Heteropolytungstates

	POM	type		W_C	W_B	W_{A1}	W_{A2}	ref
10	$P_2W_{18}O_{62}^{6-}$ [a]	III	*q*	3.646	3.597			46, 47
			δ	−128	−174			48
11	α $As_2W_{18}O_{62}^{6-}$	III	*q*	3.681	3.636			49
			δ	−121.9	−145.3			48
12	*γ**-$As_2W_{18}O_{62}^{6-}$	*γ**III	*q*	3.683	3.629			49
			δ	−110	−166			48
13	A-*β*-$Si_2W_{18}Ti_6O_{77}^{14-}$	IV	*q*	3.683	3.617			50
			δ	−132	−146			
14	$[Sb_2W_{18}Zn_3(H_2O)_3]^{12-}$	V	*q*	3.677	3.704			57
	$[Sb_2W_{18}Na_3Zn_3(H_2O)_3]^{9-}$		*q*	3.673	3.667			
	sodium added		*δ*	−97	−148			
15	$NaP_5W_{30}O_{110}^{14-}$	VI	*q*	3.567 (W_{B1})	3.560 (W_{B2})	3.543	3.521	58
			δ	−208	−210	−276	−288	48

[a] Averaged for two structures.

important role in the chemical shift. Decreased charges for the cap C and belt B tungsten atoms correspond to increased shielding for tungsten in the Dawson anion, while the shielding for the W_B atoms is larger due to the presence of the three corner-sharing oxygen atoms.

In case of $[As_2W_{18}O_{62}]^{6-}$, the structures of α and *γ** isomers have been solved by Neubert and Fuchs.[49] The second anion differs from the Dawson α structure by the 60° rotation of two polar triplet caps followed by the 60° rotation of one of the new (AsW_9O_{31}) units along the 3-fold axis, giving rise to centrosymmetric anion. Two equivalent caps and belts give a two-line 1:2 pattern in the ^{183}W NMR spectrum, whose chemical shifts are consistent with the calculated charges (Table 3).

There is a whole series of dimeric anions formed by the Keggin anion XW_9O_{33}, where three tungsten atoms are replaced by low valent cations and the former terminal oxygen atoms act as bridges between two units with formation of, for example, [A-*β*-$Si_2W_{18}Ti_6O_{77}$]$^{14-}$ (Figure 3).[50] As the ^{183}W NMR spectrum shows, the tungsten atoms in belts are more shielded than those in the rotated triplets. (Note $^2J_{W-O-W}$ =15.5 Hz.) The chemical shifts −132 ppm (triplet) and −146 ppm (belt) are consistent with the calculated charges 3.683 and 3.617, respectively. The

structure of another isomer [A-α-$Ge_2W_{18}Ti_6O_{77}$]$^{14-}$ has been determined by Yamase et al.,[51] and the ^{183}W NMR spectrum is measured. Similar to the β isomer, the charge on tungsten in the triplet is higher (3.670) than that on the belt tungsten, but the reverse pattern in the ^{183}W spectrum (−108 ppm for the belt and −128 ppm for the triplet) may point out some changes that occur upon dissolving the salt. Unfortunately, the value of $^2J_{W-O-W}$ coupling equal to 17.4 Hz is in the usual range of the interaction through corner sharing for both α and β isomers (see, for example, [β−$GeW_{12}O_{40}$]$^{4-}$; $^2J_{W-O-W}$ is 20.5 Hz).[52,53] Trimetallo (Al or Ga) derivatives of lacunary 9-tungstosilicates both α and β forms give very close $^2J_{W-O-W}$ values (15.3−15.9 Hz).[54] However, for the α-substituted complex [A-α-$P_2W_{21}O_{71}(H_2O)_3$]$^{6-}$, the value $^2J_{W-O-W}$ for triplet and belt interactions is 22 Hz.[55]

Thus, it could be assumed that the reversed pattern in the ^{183}W spectrum may result from several factors and one of them is the most probable: splitting the dimer into monomers, and in this case, the inverse two-line pattern could be observed similar to one found by Finke et al.[56] for [A-β-$Si_2W_{18}Nb_6O_{77}$]$^{8-}$ → [A-β-$SiW_9Nb_3O_{40}$]$^{7-}$.

In another dimeric anion similar to **III** but with the triplets (W_C) removed, two halves are combined by three addenda atoms, for example, [B-$Sb_2W_{18}Zn_3(H_2O)_3$]$^{12-}$ (Figure 3) studied by Kortz et al.[57] The authors underline that the anion contains three sodium cations located in the mirror plane formed by three Zn atoms firmly bound to the anion. From calculation of the charges, it may be deduced that those sodium atoms are bound to the anion in solution. The calculated charges for the triads (W_A) and belts (W_B), when the anion lacks sodium atoms, do not correspond to the observed pattern in the ^{183}W spectrum (Table 3), and only with the addition of sodium atoms at three equivalent positions in the mirror plane are the calculated charges consistent with the observed trend.

Another representative of the Keggin derivative is large POM [$NaP_5W_{30}O_{110}$]$^{14-}$ (**IV**) (Figure 3) with unusual 5-fold symmetry, which gives rise formally to two different sets of tungstens.[58] Five fragments (shown as shaded octahedra) of the Keggin anion are combined by corners resulting in formal D_{5h} symmetry, but the presence of nonlabile Na^+ on the 5-fold axis above the pseudomirror plane that contains the five phosphorus atoms gives rise to the four-line pattern with the intensity ratio 2:2:1:1 in the ^{183}W NMR spectrum.[48] Calculation of the charges on the tungsten atoms reveals that the electron density on the tungstens W_A and W_{A1} near the opening is larger, corresponding to their shielding. In the crystal structure, determination of the sodium occupies two positions with 0.5 probabilities. Placing sodium in one part of the whole anion results in a notable decrease of the charge (0.022) on polar W_A tungsten atoms. Consequently, we may attribute the most negatively shifted line to these types of tungsten atoms. It is noteworthy that these tungsten atoms (W_A) are linked by four corner-sharing oxygen atoms.

Generally speaking, a distinct trend in the chemical shifts and the charges is observed for the POM considered. In the Lindqvist structure **I**, the tungsten atoms have four oxygen atoms in the *xy* plane that form edge sharing, resulting in the largest chemical shift. Then, replacing these oxygen atoms by corner-sharing ones gives rise to gradual shielding (**I**, **Ia** (W_B), **II**, **III** (W_B), and **IV**(W_B)), and at the same time the charge on the tungsten atoms decreases, as well. Thus, the corner oxygen atoms generally induce a larger decrease of the charge on tungsten atoms, if compared with the edge shared type, due to better interaction.

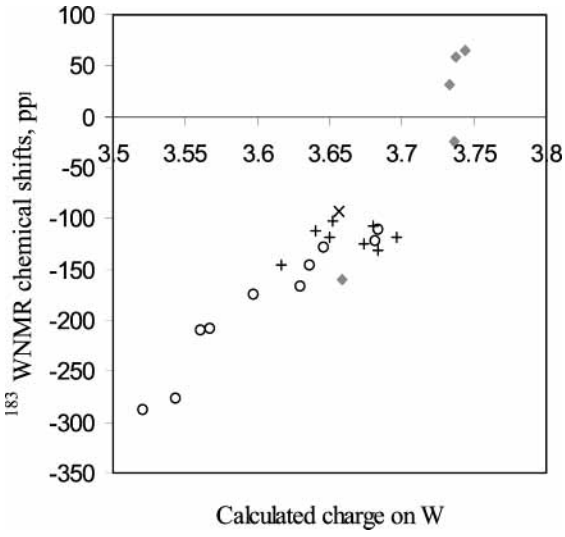

Figure 4. Plot between the ^{183}W NMR chemical shifts and the calculated charges on tungsten in different POM: ◆, anions 1−5; +, anions 6−9; ○ anions 10−15. All anions are from Tables 1−3.

The calculated charge (3.562) on W in WO_3 (where all octahedra have corner sharing), corresponds to the observed chemical shift (−200 ppm), supporting the observed trend in the chemical shift/the calculated charge.

In Figure 4, the ^{183}W NMR chemical shifts are plotted against the calculated charges on the corresponding tungsten atoms. Thus for the considered anions, we may observe a fair correspondence between the ^{183}W NMR chemical shifts and the charges on tungsten. The plot allows a change of the chemical shift to be estimated, if all bond lengths in POM, for example, $[W_6O_{19}]^{2-}$, are slightly enlarged for 0.5% ($R_{W=O}$ increased from 1.7000 to 1.7085 Å). The calculated charge on W in this case increases from 3.756 to 3.779, corresponding to an increased chemical shift by 31 ppm. By this, we would like to underline that the chemical shift is extremely sensitive to the local oxygen environment and that using the optimized POM structures may result in somewhat erroneous conclusions.

However, we should mention that for certain POMs some discrepancies in the general trend chemical shift/charge are observed. For example, for the Keggin anions [α-$XW_{12}O_{40}$]$^{n-}$, the calculated charge on tungsten decreases in a series X= P(V), Si (IV), H_2^{2+} (Table 4),[27,59−61] which is consistent with the increasing shielding. However, for [$BW_{12}O_{40}$]$^{5-}$ and [$AlW_{12}O_{40}$]$^{5-}$ anions,[62,63] the calculated charges are greater, which might assume the larger chemical shifts than for phosphotungstate. It means that some modification of the structure (sort of shrinking) happens upon dissolving (when adopting effective symmetry T_d) and the bridging oxygen atoms in the borotungstate may actually interact more strongly (increasing LUMO energies), than that it follows from the crystal data. It should be noted as well that the band in the IR spectrum assigned to vibrations of the bridging W−O−W is observed at a higher frequency than in phosphotungstate, which also correlates with larger ΔE. Similar consideration may be applied to [α-$AlW_{12}O_{40}$].[5−63,64] Such difficulties may be encountered, when calculating the chemical shifts by modern techniques.

The Keggin anion may exist in several isomeric forms, and the structures may differ by the number of the triplets rotated around the C_3 axis for 60°, β isomer when one triplet ($3W_C$) is rotated (β-**II**) and γ isomer (γ-**II**) with two rotated triplets (Figure 2). In the β isomer (β-**II**), rotation of the one triplet (shaded octahedra) reduces high symmetry of the Keggin anion from T_d to C_{3v}, resulting in three types of tungsten atoms C, B,

TABLE 4: Charges on Atoms and the ^{183}W NMR Chemical Shifts in the Keggin Anions and Its Isomeric Forms

	POM	charge shift, ppm	W_A	W_B	W_C	W_D	ref
16	$SiW_{12}O_{40}^{4-}$	*q*	3.652[a]				56, 60
		δ	−103				12
17	$H_2W_{12}O_{40}^{6-}$	*q*	3.623 (3.584)				61
	($W_{12}O_{40}^{8-}$)	δ	−112				12
18	$BW_{12}O_{40}^{5-}$	*q*	3.688[b] (3.629)				62
	($Na_2BW_{12}O_{40}^{3-}$)	δ	−130				12
19	$AlW_{12}O_{40}^{5-}$	*q*	3.691				63
		δ	−112.8				63, 64
20	β-$SiW_{12}O_{40}^{4-}$	*q*	3.726	3.669	3.737		59, 65, 66
		δ	−130	−115	−110		7, 8
21	γ-$SiW_{12}O_{40}^{4-}$	*q*	3.793	3.691	3.683	3.672	67
		δ	−160	−105	−117	−127	68

[a] Average value from two X-ray crystal works. [b] Average value for two types of the anion having C_2 and D_2 symmetries in a single crystal.

and A (C rotated triplet), and such an isomer is characterized by the three-line pattern in ^{183}W NMR spectra with the intensity ratio 1:2:1 (C:B:A).[7,8] The structure of the [β-$SiW_{12}O_{40}$]$^{4-}$ has been studied in three works.[59,65,66] Though French authors[66] had worked on the mixed addenda anion [β-$SiMoW_{11}O_{40}$]$^{4-}$, where one molybdenum statistically replaces tungsten supposedly in the triad (W_A), they give more accurate data. The calculated charges averaged for three structures and the observed chemical shifts are presented in Table 4. The calculated charges for tungsten in the rotated triplet and in the corner-shared triad are proven to be larger than those for the six-tungsten belt. The larger chemical shift for the tungsten (W_C) in the rotated triplet corresponds to the larger calculated charge, but at present the increased charge for tungsten in the triad (W_A) cannot be explained. We can mention that despite very close properties of Mo(VI) and W(VI), the molybdenum may influence the bond lengths of tungsten both in the six-tungsten belt and triad. It could be that the bond lengths in those octahedra of the triad, which are slightly shorter than those found in the crystal structure determination and dissolution of the salt, may result in the relaxation of some bonds giving the observed NMR pattern. Or, the increase in ΔE results in a strong decrease in the paramagnetic contribution and despite increased charge the observed chemical shift is the least.

The third γ isomer of the Keggin anion [γ-$XW_{12}O_{40}$]$^{n-}$ (γ-**II**) with two rotated triplets has C_{2v} symmetry with four different types of tungsten atoms (Figure 2).[67] Two W_A atoms have a common edge in the formal *xy* plane (local *z* axis coincides with a bond W═O and actually can be viewed as being a square pyramid, because the oxygen atoms common with Si are too far from W_A. The ^{183}W NMR spectrum of [γ-$SiW_{12}O_{40}$]$^{4-}$ measured by Tézé et al.[68] shows the expected 4:1:4:1 pattern.

However, the lowest chemical shift for W_A falls out of the expected trend. The charge is the highest for W_A, which is not surprising because, as it follows from the calculation, the less oxygen atoms in the polyhedron around tungsten, the higher positive charge. However, the chemical shift assigned to these tungstens in the structure of [γ-$SiW_{12}O_{40}$]$^{4-}$ indicates that they are the most shielded. The situation cannot be explained until the actual calculation of the paramagnetic shifts is done for such a case. Positions of the other three lines in the ^{183}W NMR spectra are fully consistent with the suggested scheme of the chemical shift vs the charge within this polyanion.

Finally, taking into account the aforementioned correlation, we may consider as an example the lacunary Keggin anion, which acts as a tetradental ligand toward lead in the unique complex [$Pb(GaO_4)W_{11}O_{35}$]$^{7-}$ and has a fixed orientation in the crystal,[69] and therefore the configuration around each tungsten atom is determined. Though no NMR spectrum is measured for this anion, for a similar complex [$Pb(PO_4)W_{11}O_{35}$]$^{5-}$, the ^{183}W NMR spectrum with complete assignment is measured,[70] and according to our EHMO calculation, the charges on tungstens are consistent with general trend excluding the values *q* for W_1 and W_6

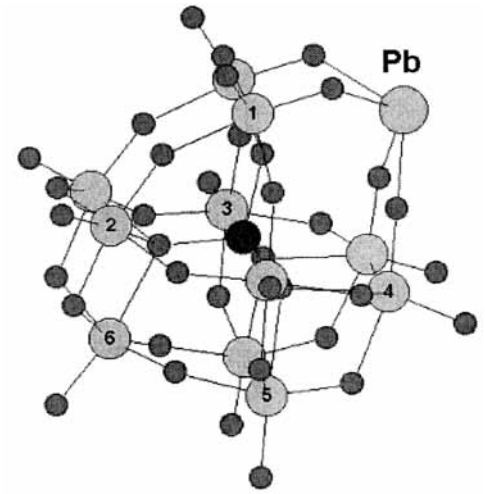

		W_1	W_4	W_5	W_6	W_3	W_2
[$Pb(GaO_4)$-$W_{11}O_{35}$]$^{7-}$	*q*	3.682	3.735	3.717	3.741	3.694	3.681
[$Pb(PO_4)$-$W_{11}O_{35}$]$^{5-}$	δ	−74.4	−88.7	−102.8	−111.5	−127.4	−146.3

However, inspection of the bond lengths reveals that the W_1−O bond in bridging W_1−O−Pb is shorter (1.76 Å) than the usual bridging bond and the terminal W$_6$═O bond (1.80Å) is too long. Allowing the former for 1.86 Å and the latter for 1.75 Å results in the charges 3.722 and 3.702, respectively, which are fairly consistent with the general trend.

Some other examples of more complex anions are given in Table S4 and Figure S2 (Supporting Information), where some necessary adjustment of the bond lengths should be made, which may prove to be useful in the calculation of the paramagnetic shielding for large POM by sophisticated methods.

As it was mentioned above, the supposed penta-coordination around tungsten W_A in [γ−$XW_{12}O_{40}$]$^{n-}$ results in increasing its charge. On the contrary, an addition of the seventh oxygen atom as observed in peroxophosphotungstate [PW_2O_{14}]$^{3-}$, where there are two peroxo groups lying in the plane perpendicular to the W═O around each tungsten atom,[71] markedly decreases the charge (3.280) corresponding to the highest shielding (−676 ppm in aqueous solution and, correspondingly, −627 ppm in acetonitrile) in the ^{183}W NMR spectrum for this tungsten (VI).

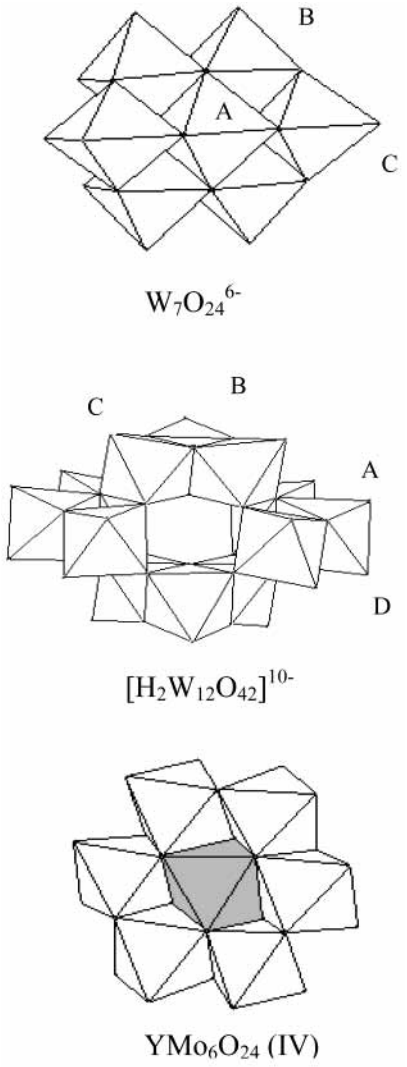

Figure 5. Structures of heptatungstate, dodecatungstate, and hexamolybdometalate.

Another group refers to two POM with octahedra having two cis $^{O}_{O}\gg$W, whose symmetry is close to C_{2v}, and it is hardly possible to expect that the calculated charges will be in the line shown in Figure 4, since the system of the magnetic dipole-allowed transitions may be different from that for POM consisting of the octahedra with C_{4v} symmetry.

The largest spread in the chemical shifts is observed for heptatungstate $[W_7O_{24}]^{6-}$ (Figure 5), with its three lines[72,73] whose intensity ratio 1:4:2 corresponds to structurally nonequivalent tungsten atoms.[74,75] The unique tungsten W_A in the middle of the anion has formally no terminal oxygen atoms, and the observed line corresponds to the most deshielded tungsten for W(VI). At the same time, the calculated charge is the highest on this tungsten atom. The other lines correspond to more shielded tungsten atoms, and the electron population on them gradually increases as follows

		W_A	W_B	W_C
$W_7O_{24}^{6-}$	q	3.893	3.730	3.720
	δ	268	−106	−189

Similar distribution of the charges was found in the DFT calculation of this anion.[76]

Dodecatungstate $[H_2W_{12}O_{42}]^{10-}$ (Figure 5) consists of four groups of different tungsten atoms,[77] and its structure is retained in solution, as confirmed by ^{183}W NMR spectrum with four lines with intensity ratio 1:2:1:2.[72,73] Two types of tungsten atoms W_A and W_D with local symmetry close to C_{2v} with two terminal oxygen atoms, give rise to the two most spaced lines. The calculated charges and the observed chemical shifts are distributed in the following manner

		W_A	W_B	W_C	W_D
$H_2W_{12}O_{42}^{-10}$	q	3.722	3.722	3.711	3.639
	δ	−109	−114	−116	−147

Calculation shows that they have the most different charges on atoms. The closely spaced two lines in the middle of the spectrum correspond to two types of tungsten atoms with local symmetry close to C_{4v}, and at the same time the charges on the tungsten atoms are only slightly different. It should be noted that, namely, these lines are inverted with decreasing pH.[73]

For both anions, the larger positive charges on tungsten having two cis terminal bonds are observed than those for POM with tungstens with one terminal bond, despite larger negative anionic charge per tungsten. It is not surprising, since octahedra in the formers are slightly swelled, and as we have mentioned above, expanding an octahedron results in increasing the positive charge on this tungsten. Nevertheless, for such anions, correspondence between the calculated charges and the ^{183}W chemical shifts and the increased charge is observed as well.

Therefore, combination of NMR data and calculation of the charges by means of EHMO and using the experimental atomic coordinates may help in assigning the observed lines, clarify the situation with the charge delocalization throughout the anion as proposed by Klemperer,[7] and establish in some cases the accuracy of the X-ray structure determination, especially for the metal cations located in the symmetry equivalent sites.

^{95}Mo NMR Chemical Shifts. In the case of polyoxometalates, ^{95}Mo NMR is not as abundant as ^{183}W NMR. For three main types **I**, **II**, and **III** similar to polytungstates (Figures 1 and 2), NMR and X-ray structure data are available. The calculated charges on molybdenum and ^{95}Mo NMR chemical shifts are given in Table 5.[46,77−80] For these three cases, it is clearly seen that increasing the calculated charge on molybdenum corresponds to increasing the chemical shift,[81,82] the trend similar to that found for the corresponding polytungstates. For $[P_2Mo_{18}O_{62}]^{6-}$ (**III**) with the Dawson structure[46] (Figure 2), the molybdenum atoms in the triplet caps bear a higher charge than ones in the belts, but for comparison, the weight average value is used because in the ^{95}Mo spectrum only a wide single line is observed.[81]

TABLE 5: ^{95}Mo NMR Chemical Shifts and the Calculated Charges

	POM	type	q_{Mo}	δ, ppm	ref
22	$Mo_6O_{19}^{2-}$	I	3.767	122	81, 77
23	$PMo_{12}O_{40}^{3-}$	II	3.713	22	78, 82
24	$P_2Mo_{18}O_{62}^{6-}$	III	3.685	−35	46, 83
25	$IO_6Mo_6O_{18}^{-5}$	IV	3.801	−11	81, 82
26	$TeO_6Mo_6O_{18}^{-6}$	IV	3.806	10	80, 82

In the Anderson-type anions $[Y^{x+}Mo_6O_{24}]^{n-}$ (where Y = Te(VI) or I(VII)) (Figure 5), the octahedra MoO_6 may be considered to have C_{2v} symmetry with two cis terminal bonds.[79,80] Similar to tungstates with octahedra of C_{2v} symmetry, the higher positive charge is built up on molybdenum in comparison with one for Mo in octahedra with C_{4v} symmetry. Some other examples of polyoxomolybdates with possible assignments of the lines for different structures are given in Table S5 and Figure S2 (Supporting Information).

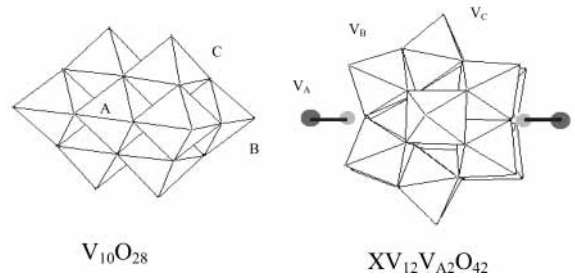

Figure 6. Structures of decavanadate and $XV_{12}V_{A2}O_{42}$.

^{51}V NMR Chemical Shifts. For polyoxovanadates, three structures without unequivocal assignment of the observed lines will be considered; one is decavanadate $[V_{10}O_{28}]^{6-}$ (Figure 6),[83,84] where three types of vanadium give a three-line pattern in the ^{51}V NMR spectrum,[85] and the other is the heteropolyvanadates $[PV_{12}V_2O_{42}]^{9-}$ (1:4:2 pattern)[86−88] and $[VV_{12}V_2O_{42}]^{9-}$, having bicapped Keggin structure (Figure 6) (four line pattern).[89]

As previously found for $[W_7O_{24}]^{6-}$, in $[V_{10}O_{28}]^{6-}$, the atom V_A having no terminal oxygen atoms is the most deshielded and it has the highest charge

	V_A	V_B	V_C
$[V_{10}O_{28}]^{6-}$	3.415	3.290	3.294
shift, ppm	113	36	21

The charges for two other types are less than for V_A, as expected, though the charges for V_B and V_C are inconsistent with the observed trend (the same spread of the charges is found in ab initio calculations),[90] but the difference is rather small and probably some changes in geometry happen upon dissolving the solid that modifies expected pattern in the ^{51}V spectrum.

On the other hand, for POM $[PV_{12}V_2O_{42}]^{9-}$ and $[VV_{12}V_2O_{42}]^{9-}$, the increasing charges is consistent with increasing ^{51}V chemical shifts of the three types of vanadium forming a coordination sphere (excluding V in the inner tetrahedron).[86−89] However, despite rather large positive charges on vanadium, the lines are strongly negatively shifted, possibly due to large negative anionic charge

	V_A	V_B	V_C
$[PV_{12}V_2O_{42}]^{9-}$	3.446	3.298	3.294
shift, ppm	21	−38	−54
$[VV_{12}V_2O_{42}]^{9-}$	3.363	3.276	3.263
shift, ppm	34	−43	−56

Calculated charges and the ^{51}V NMR chemical shifts with possible assignments for other POM containing vanadium are given in Table S6 and Figure S2 (Supporting Information).

3. NMR and Diamagnetic POM with Localized and Delocalized Electron Density

Many of the considered POM built up of octahedra with one terminal bond W═O may be reduced by one, two, and more electrons without changing the initial structure,[1−5] and it is relevant to consider NMR and calculated data for large polyanions, which contain the introduced electrons. In most cases, two electrons are delocalized and paired allowing metal NMR spectra to be measured in solution.[5] Depending on structure, the electron pair (bipolaron) may be delocalized over the whole framework of the coordination sphere or part of it. On the other hand, the introduced electrons may localize on specific metal atom(s) due to forming the metal−metal bond, especially, when the oxygen is replaced by sulfur as in $[\gamma\text{-}SiW_{12}S_2O_{38}]^{6-}$. The ^{183}W NMR may reveal the atoms that accept electrons in the reduced species by characteristic positive shifts of their corresponding lines. As a matter of fact, in some extent, this contradicts the general rule according to which decreasing the oxidation state results in larger shielding due to the presence of electrons, and therefore, the line shifts to high field.[91] Mostly it refers to the mononuclear complexes, and on the contrary, if the complex is dimer with metal−metal bond formed, the resonance line shifts to low field, showing larger deshielding with decreasing the oxidation state.[92] Such a deshielding is explained by availability of low-lying empty orbitals in a metal−metal bond inducing large paramagnetic electron circulation, giving a positive shift. Thus, it would be interesting to carry out calculation on reduced species to find, first, how the charges change during reduction and to see which cations accept electrons.

According to electron spin resonance data, a single electron introduced into $[\alpha\text{-}SiW_{12}O_{40}]^{4-}$ is evenly delocalized over the coordination sphere.[93] The second introduced electron is completely paired with the first one, and this electron pair (bipolaron), according to NMR, is also delocalized.[94] The difference in charges on tungsten between the oxidized and reduced species shows a fraction of electron density on each cation (Table 6). At the same time, the positive shift (60 ppm) of the ^{183}W line is observed,[94] revealing uniform distribution of the introduced electron pair over the coordination sphere.

The preferential delocalization of the electron pair over the belt in $[P_2W_{18}O_{62}]^{6-}$ is clearly seen by the shift of the line assigned to the belt tungsten atoms (W_B) (Figure 3).[94] At the same time, calculations show decreasing the positive charge on tungsten atoms of the belt as well (Table 6). Calculation also reveals that nondegenerate HOMO, occupied by two electrons, is comprised of 12W $5d_{xy}$ orbitals (see Figure S3 of Supporting Information) and whose energy is markedly lower than one of the rest of the MO. The charge on belt tungsten atoms decreases due to the delocalized electron density, and at the same time, the tungsten in the caps do not acquire any electron density, and the charge rests the same as for the oxidized parent.

The second POM with uneven distribution of the two introduced electrons is $[W_{10}O_{32}]^{6-}$, where the electron pair is delocalized over 8 tungsten atoms W_B (Figure 1), as it is deduced from the ^{183}W NMR spectrum.[31] According to calculations, the electron density is evenly distributed in the HOMO consisting of these 8 W_B (see Figure S3 in Supporting Information). A small positive shift of the line attributed to the apical atoms may be explained by a slightly enlarged octahedron in the reduced state[28] (the calculated charge on these W_A is larger than that for the nonreduced anion) and definitely not by delocalization of the electrons on the two apical tungstens. Decreasing the number of metallic atoms acquiring electron density results in larger positive shift in the ^{183}W NMR spectrum of some lines for $[\gamma\text{-}SiW_{12}O_{40}]$.[6−67,68] The difference between calculated charges for the initial and reduced forms points out preferential distribution of the electron pair over four neighboring tungstens W_D with partial delocalization over other tungsten atoms that is fairly consistent with interpretation of NMR spectrum. According to calculation, LUMO accepting two electrons is composed of the atomic orbitals, namely, of these tungsten atoms (see Figure S3 of Supporting Information) like it was found in DFT calculation.[95] On the contrary, in $[\gamma\text{-}SiW_{12}S_2O_{38}]^{6-}$, where two adjacent W_A have sulfide S^{2-}, as bridging atoms forming strongly stabilized HOMO (electron sink), the two electrons completely reside on them due to the metal−metal bond.[96] No electron transfer occurs in this case on the neighboring atoms. The decrease of the calculated charge

TABLE 6: ^{183}W NMR of Mixed Valence Anions and Charges on Cations, Received Electron Density

		$M_{A(D)}$		M_B		M_C		
	POM	*q*	*δ*	*q*	d	*q*	d	ref
1	$SiW_{12}O_{40}^{6-}$	0.078	60					94
2	$P_2W_{18}O_{62}^{8-}$			0.16	126			94
3	$W_{10}O_{32}^{6-}$			0.243	410			31
4	γ-$SiW_{12}O_{40}^{6-}$	0.381	617	0.081	42	0.013	37	67, 68
5	$ON-W_6O_{18}^{3-}$	0.694	594					106
6	β $-SiW_{12}O_{40}^{6-}$	0.132		0.164		0.214		
7	γ- $SiW_{12}S_2O_{38}^{6-}$	0.858	1218					96
8	$BW_{12}O_{37}(OH_2)_3^{5-}$(6e)	1.477	1542					62
	β $-SiMo_{12}O_{40}^{6-}$	0.192		0.153		0.146		101, 102
9	β $-PMo_{12}O_{40}^{7-}$ q	0.333		0.308		0.331		103
	^{17}O NMR shift [q][δ]	−1.347	915	−1.340	933	−1.365	911	103, 104

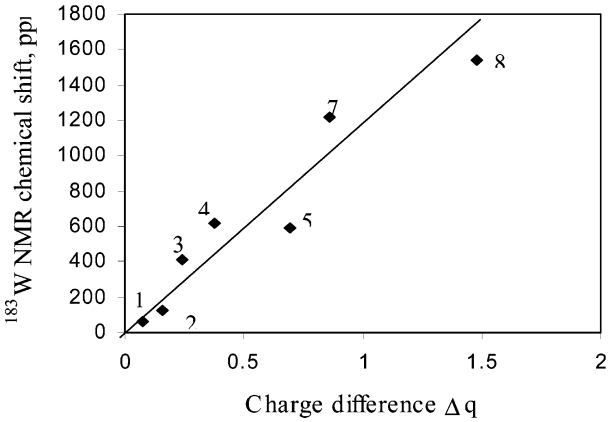

Figure 7. Correlation between the ^{183}W NMR chemical shifts and the charge difference.

in this case is the greatest for d^1 complexes. A similar situation is observed when two W_A atoms are replaced by Mo_A and introduced electrons reside on molybdenum atoms, since LUMO consisting of d_{xy} orbitals of Mo in the oxidized anion, is markedly stabilized in comparison with the orbitals formed mostly by tungsten.

Reduction of the Keggin anion by six electrons results in complete localization of electron density on three tungsten atoms in the triplet group with reduced W(IV) forming a metal−metal bond.[97] Such a configuration strongly deshields the corresponding tungsten atoms, and the line is observed around 1500 ppm.[98] Gradual increase of the chemical shift is observed as well with decrease of the oxidation state and the largest shift (6700 ppm) is observed for dimeric $W_2(O_2CF_3)_4$ with W(II) where closely spaced δ orbitals form.[99]

Correlation between the differences in the calculated charges for oxidized and reduced species and the chemical shifts (Figure 7) clearly shows the principal role of the paramagnetic contribution to the observed chemical shifts due to circulation of the introduced electrons.

Unfortunately, there is still no data on NMR for reduced $[\beta\text{-}XW_{12}O_{40}]^{n-}$. Calculated charges, when two electrons are introduced into $[\beta\text{-}XW_{12}O_{40}]^{n-}$ using oxidized structure, show delocalization of slightly larger electron density over the triad (Table 6). It should be noted that, if we use averaged geometry in strict symmetry C_{3v}, the belt tungsten atoms acquire electron density in a greater extent, but conclusion strongly depends on the bond lengths in the bridges W_A-O-W_B and W_B-O-W_C between the belt and triad and triplet. As a matter of fact, calculations on $[\beta\text{-}SiMo_{12}O_{40}]^{6-}$ reduced with two electrons, whose structure is determined recently,[100] show larger electron density on molybdenum atoms of the rotated triplet C (Figure 2 and Table 6). The interesting issue is the distribution of four electrons in $[\beta\text{-}PMo_{12}O_{40}]^{7-}$, whose structure were solved in two studies.[101,102] Calculated charges show that electron density is almost uniformly distributed over anion, though slightly larger on the triplet and the triad. Indirectly, such a distribution may be confirmed by ^{17}O NMR spectra of the reduced forms, where the smaller negative calculated charge on the terminal oxygen atoms corresponds to larger shifts (Table 6).[103,104] Unfortunately, ^{95}Mo NMR spectrum cannot give unequivocal answer on distribution of four electrons.[105] Two wide lines observed at +800 and −200 ppm approximately of equal intensities may correspond to either delocalization of each electron pair in triplet and triad (giving +800 ppm shift) separated by the six tungsten belt (−200 ppm), corresponding to larger calculated charges, or four electrons may be delocalized over the belt. In both cases the line, corresponding to molybdenum atoms that do not accept electrons, is assumed to be negatively shifted similar to case of $[P_2W_{18}O_{62}]$,$^{6-}$ where the line of the belt tungstens accepting electrons is positively shifted and one of the caps is strongly negatively shifted.[94] We may assume that for anion in solution with relaxation of some bond length, repulsion of two electron pairs may favor their separation in triplet and triad (corresponding lines may be overlapped), moreover protonation of the bridging oxygen atoms in the belt may hamper delocalization in the belt.

Some words should be said about the nitrosyl complex $[W_5O_{18}W-NO]^{3-}$, where the oxidation state of W in the W−N−O fragment is considered to be 2 + (d^4).[106] This tungsten is proved to be strongly deshielded[106] and according to calculation bears lower charge than the rest tungsten atoms. The chemical shift correlates with the charge difference corresponding to localization approximately of one electron on the W linked to ligand NO group (Table 6), and the rest of the electron density is delocalized over NO group with small participation of d_π orbitals (see Figure S6 of Supporting Information). Formally, the d_{xy} orbital of W_A is vacant, and despite this, there is some delocalization of electron density over neighboring atoms as may be deduced from NMR. Probably in the excited state, electron density is actually transferred and calculation shows that in this case the charge on tungstens reduced.

4. Conclusions

Having calculated the charges on atoms forming the coordination sphere and comparing them with the corresponding chemical shifts for a large number of POM, we may see that there is a definitive correlation between these two values. The stronger interaction between oxygen and metal of the coordination sphere, the less positive charge on this cation that is accompanied by increasing energy gap between bonding and antibonding MO and, consequently, the nucleus under study is more shielded. It is hoped that more detailed information will be obtained in real calculations of the shielding, but as a

preliminary test of the structure that will be calculated, the EHMO method can be used to get the first approximation. It was shown that Σ ($1/\Delta E$) where summation is done for five inverse energy separations between the bonding MO and five virtual d* orbitals calculated by EHMO not only for individual octahedron taken from the structure but also using baricenters of the bonding and virtual five MO calculated for the whole anions may be fairly correlated with the chemical shift.[35] An increase in the electronic population on a nucleus surrounded by the same ligands (in our case, oxygen) coincides with a general trend in metal NMR shift. Even small changes of the charge may influence not only the metal chemical shifts but also the ^{31}P NMR chemical shifts in the heteropolyanions (see Supporting Information, Table S7 and a plot in Figure S4 between the chemical shift and the charge difference calculated for phosphorus in HPA and on phosphorus in PO_4 isolated from the same anion, showing influence of the coordination sphere on the phosphorus charge).

Drastic negative shift of the NMR line, for example, in mononuclear complexes with decreasing the oxidation state (increase of electron population), is well known.[91] However, reduction of POM with two electrons or with six electrons results in large positive shift, despite marked decrease of the charge.[5] This is characteristic of dimer complexes with the metal−metal bonds and deshielding increases with an increase of metal−metal bond order.[92] Namely paramagnetic circulation of the electrons within metal−metal bonding induces large deshielding. Therefore, it will be a challenge to calculate the shielding in such complexes.

Accuracy of the calculation may strongly depend on an adopted geometry, when averaging of the bonds and angles between them are made, and therefore quick and easy testing of the analyzed structure will be desirable and EHMO is suitable for such an approach. Another possibility to use EHMO for understanding the chemical shift is to find possibility to calculate the magnetically dipole-allowed transitions such as is has been done for interpretation of the electronic transitions.[107] Moreover, POM is very suitable object to verify some theories that are used in calculating the NMR chemical shift of nuclei comprising a polyoxoanion. At the same time these calculations should be compared with other physicochemical data to get consistent conclusion, especially much caution should be undertaken in considering the mixed POM.

Acknowledgment. Authors thank Prof. I. Kawafune, K. Nomya, and J. Errington for sending detailed structural information and Prof. A. Bagno for the preprint before publication. L.P.K. highly appreciates the fellowship from JSPS.

Supporting Information Available: Tables documenting electronic population on tungsten, molybdenum, and vanadium, ionization potentials, coefficients, and exponents of EHMO calculations, chemical shifts and calculated charges for ^{183}W, ^{95}Mo, and ^{51}V, ^{31}P NMR chemical shifts and figures showing a plot between the ^{183}W NMR chemical shifts and charge on tungsten, structures of dimeric polytungstates, polymolybdates, and methylated hexavanadate, HOMO for the reduced polyanion, and dependence between the ^{31}P NMR chemical shidts and the difference of the charges on phosporus. This material is available free of charge via the Internet at http://pubs.acs.org.

References and Notes

(1) Pope, M. T. *Heteropoly and Isopoly Oxometalates*; Springer: Berlin, 1983.
(2) *Polyoxometalates: from platonic solids to anti-retroviral activity*; Pope, M. T., Müller, A., Eds.; Kluwer: Dordrecht, 1994.
(3) Pope, M. T.; Müller, A. *Angew. Chem., Int. Ed. Engl.* **1991**, *30*, 34−48.
(4) Baker, L. C. W.; Glick, D. C. *Chem. Rev.* **1998**, *98*, 3.
(5) Kazansky, L. P.; McGarvey, B. R. *Coord. Chem. Rev.* **1999**, *188*, 157.
(6) Mason, J. Ed. *Multinuclear NMR*; Plenum: New York, 1987.
(7) Gansow, O. A.; Ho, R. K. C.; Klemperer, W. G. *J. Organomet. Chem.* **1980**, *187*, c27.
(8) Lefebvre, J.; Chauveau, F.; Doppelt, P.; Brevard, C. *J. Am. Chem. Soc.* **1981**, *103*, 4589.
(9) Sveshnikov, N. N.; Pope, M. T. *Inorg. Chem.* **2000**, *39*, 591.
(10) Kazansky L. P. *Chem. Phys. Lett.* **1994**, *223*, 289.
(11) Mason, J. *J. Am. Chem. Soc.* **1991**, *113*, 24.
(12) Acerete, R.; Hammer, C. F.; Baker, L. C. W. *J. Am. Chem. Soc.* **1982**, *104*, 5384.
(13) Kazansky, L. P.; Chaquin, P.; Fournier, M.; Herve, G. *Polyhedron* **1998**, *26*, 4353.
(14) Combariza, J. E.; Barfield, M.; Enemark, J. H. *J. Phys. Chem.* **1991**, *95*, 5463.
(15) Hada, M.; Kaneko, H.; Nakatsuji, H. *Chem. Phys. Lett.* **1996**, *261*, 7.
(16) Rodriguez-Fortea, A.; Alemany, P.; Ziegler, T. *J. Phys. Chem. A* **1999**, *103*, 8288.
(17) Ruiz-Morales Y.; Zigler, T. *J. Phys. Chem.* **1998**, *102A*, 3970.
(18) Nakatsuji, H.; Sugimoto, M.; Saito, S. *Inorg. Chem.* **1990**, *29*, 3095.
(19) Bühl, M.; Hamprecht, F. A. *J. Comput. Chem.* **1998**, *19*, 113.
(20) Bagno, A.; Bonchio, M. *Chem. Phys. Letts.* **2000**, *317*, 123.
(21) Bagno, A.; Bonchio, M.; Sartorel, A.; Scorrano, G. *ChemPhysChem.* **2003**, *4*, 4353.
(22) Clayton, T. W.; Bursten B. E. *New J. Chem.* **1991**, *15*, 713.
(23) Bühl, M.; Thiel, W.; Fleischer, U.; Kutzelnigg, W. *J. Phys. Chem.* **1995**, *99*, 4000.
(24) Rytz, R.; Calzaferri, G. *J. Phys. Chem.* **1997**, *101*, 1B, 5664.
(25) Krylov, N. I.; Kolomnikov, I. S. *Koord. Khim.* **19**77, *3*, 1895.
(26) Fuchs, J.; Freiwald, W.; Hartl, H. *Acta Crystallogr.* **1978**, *B34*, 1764.
(27) Brown, G. M.; Noe-Spirlet, M.-R.; Busing, W. R.; Levy, H. A. *Acta Crystallogr.* **1977**, *B33*, 1038.
(28) Sasaki, Y.; Yamase, T.; Ohashi, Y.; Sasada, Y. *Bull. Chem. Soc. Jpn.* **1987**, *60*, 4285.
(29) Fuchs, J.; Hartl, H.; Schiller, W.; Gelach, U. *Acta Crystallogr.* **1976**, *B32*, 740.
(30) Kazansky, L. P.; Fedotov, M. A.; Spitsyn, V. I. *Dokl. Acad. Nauk SSSR*, **1983**, *272*, 1179.
(31) Duncan, D. C.; Hill, C. L. *Inorg. Chem.* **1996**, *35*, 5828.
(32) Bridgeman, A. J.; Cavigliasso, G. *J. Phys. Chem. A* **2002**, *106*, 6114.
(33) Iball J.; Low, J. N.; Weakley, T. J. R. *J. Chem. Soc., Dalton Trans.* **1974**, 2021.
(34) Ozeki T.; Yamase, T. *Acta Crystallogr.* **1994**, *B50*, 128.
(35) Inoue, M.; Yamase, T.; Kazansky, L. P. *Polyhedron* **2003**, *22*, 1183.
(36) Clegg, W.; Elsegood, M. R. J.; Errington, R. J.; Havelock, J. *J. Chem. Soc., Dalton Trans.* **1996**, 681.
(37) Day V. W.; Klemperer, W. G.; Maltbie, D. *J. Organometallics* **1985**, *4*, 104.
(38) Che T. M.; Day, V. W.; Francesconi, L. C.; Klemperer, W. G.; Main, D. J.; Yagasaki, A.; Yaghi, O. M. *Inorg. Chem.* **1992**, *31*, 2920.
(39) Pope, M. T.; O'Donnell, S. E.; Prados, R. A. *J. Chem. Soc., Chem. Commun.* **1975**, 22.
(40) Kazansky L. P.; Fedotov, M. A.; Ptushkina, M. N.; Spitsyn, V. I. *Dokl. Akad. Nauk SSSR.* **1975**, *224*, 1029.
(41) Kawafune, I.; Tamura, H.; Matsubayashi, G.-e. *Bull. Chem. Soc. Jpn.* **1997**, *70*, 2455.
(42) Kawafune, I.; Matsubayashi, G.-e. *Bull. Chem. Soc. Jpn.* **1996**, *69*, 359.
(43) Domaille, P. *J. Am. Chem. Soc.* **1984**, *106*, 7677.
(44) Nomya, K.; Hasegawa, T.; Noguchi, R.; Nomura, K.-I.; Takahashi, M.; Yokoyama, H. *Chem. Lett.* **2001**, 1278.
(45) Harrup, M. K.; Kim, G.-S.; Zeng, H.; Johnson, R. P.; VanDervee, D.; Hill, C. L. *Inorg. Chem.* **1998**, *37*, 5550.
(46) D'Amour, H. *Acta Crystallogr.* **1976**, *B32*, 729−740.
(47) Sergienko, V. S.; Porai-Loshits, M. A.; Kiselev, S. V.; Butman, L. A.; Chuvaev, V. F. *Z. Neorgan. Khim.* **1983**, *28*, 1199.
(48) Acerete, R.; Hammer, C. F.; Baker, L. C. W. *Inorg. Chem.* **1984**, *23*, 1478.
(49) Neubert, H.; Fuchs, J. *Z. Naturforsch.* **1987**, 42b, 951.
(50) Lin, Y.; Weakley, T. J. R.; Rapko, B.; Finke, R. G. *Inorg. Chem.* **1993**, *32*, 5095.
(51) Yamase, T.; Ozeki, T.; Sakamoto, H.; Nishiya, S.; Yamamoto, A. *Bull. Chem. Soc. Jpn.* **1993**, *66*, 103.

(52) Thouvenot, R.; Fournier, M.; Franck, R.; Rocchiccioli-Deltcheff, C. *Inorg. Chem*. **1984**, *23*, 598.
(53) Mayer, C. R.; Thouvenot, R. *J. Chem. Soc., Dalton Trans*. **1998**, 7.
(54) Liu, J.; Ortega, F.; Sethuraman, P.; Katsulis, D. E.; Costello, C. E.; Pope, M. T. *J. Chem. Soc., Dalton Trans*. **1992**, 1901.
(55) Tourné, C.; Tourné, G. F.; Weakley, T. J. R. *J. Chem. Soc., Dalton Trans.* **1986**, 2237.
(56) Finke, R. G.; Droege, M. W. *J. Am. Chem. Soc.* **1984**, *106*, 7274.
(57) Kortz, U.; Al-Kassem, N. K.; Savelieff, M. G.; Al Kadi, N. A.; Sadakane, M. *Inorg. Chem.* **2001**, *40*, 4742.
(58) Alizadeh, M. H.; Harmalker, S. P.; Jeannin, Y.; Martin-Frére, J.; Pope, M. T. *J. Am. Chem. Soc.* **1985**, *107*, 2662.
(59) Fuchs, J.; Thiele, A.; Palm, R. *Z. Naturforsch.* **1981**, *36B*, 161−171.
(60) Kobayasi, A.; Sasaki, Y. *Bull. Chem. Soc. Jpn.* **1975**, *48*, 885.
(61) Asami M.; Ichida, H.; Sasaki, Y. *Acta Crystallogr.* **1984**, *C40*, 35−37.
(62) Yamase, T.; Ishikawa, E. *J. Chem. Soc., Dalton Trans.* **1996**, 1619−1627.
(63) Weinstock, I. A.; Cowan, J. J.; Barbuzzi, E. M. G.; Zeng, H.; Hill, C. L. *J. Am. Chem. Soc.* **1999**, *121*, 4608.
(64) Fedotov M. A.; Kazansky L. P. *Izv. Akad. Nauk SSSR. Ser. Khim*. **1988**, 2000.
(65) Matsumoto, K. Y.; Kobayashi, A.; Sasaki, Y. *Bull. Chem. Soc. Jpn.* **1975**, *48* (11), 3146.
(66) Robert, F.; Tezé, A.; Hervé, G.; Jeannin, Y. *Acta Crystallogr.* **1980**, *36B*, 11.
(67) Tezé, A.; Cadot, E.; Béreau, V.; Hervé, G. *Inorg. Chem.* **2001**, *40*, 2004.
(68) Tezé, A.; Canny, J.; Gurban, L.; Thouvenot, R.; Hervé, G. *Inorg. Chem.* **1996**, *35*, 1001.
(69) Tourné, G. F.; Tourné, C. M.; Schouten, A. *Acta Crystallogr.* **1982**, *B38*, 1414.
(70) Brevard, C.; Schimpf, R.; Tourné, G.; Tourné, C. *J. Am. Chem. Soc*. **1983**, *105*, 7059.
(71) Salles, L.; Aubry, C.; Thovenot, R.; Robert, F.; Doremieux-Morin, C.; Chottard, G.; Ledon, H.; Jeannin, Y.; Bregeault, J.-M. *Inorg. Chem*. **1994**, *33*, 871.
(72) Maksimovskaya, R. I.; Burtseva K. G. *Polyhedron* **1985**, *4*, 1559.
(73) Hastings, J. J.; Howarth, O. W. *J. Chem. Soc., Dalton Trans.* **1992**, 209.
(74) Fuchs, J.; Flint, E. P. *Z. Naturfosch.* **1979**, *34B*, 412.
(75) Bridgeman, A. J.; Cavigliasso, G. *J. Chem. Soc., Dalton Trans.* **2002**, 2244.
(76) Evans, H. T. *J. Am. Chem. Soc.* **1983**, *105*, 4839.
(77) Nagano, O.; Sasaki Y. *Acta Crystallogr.* **1979**, *35B*, 2387.
(78) D'Amour H.; Allman, R. *Z. Kristallogr*. **1976**, *143*, 1.
(79) Evans, H. T. *Acta Crystallogr.* **1974**, *B30*, 2095.
(80) Kondo, H.; Kobayashi, A.; Sasaki, Y. *Acta Crystallogr*. **1980**, *B36*, 551.
(81) Masters, A. F.; Gheller, S. F.; Brownlee, R. T. C.; O'Connor, M. J.; Wedd, A. G. *Inorg. Chem.* **1980**, *19*, 3866.
(82) Fedotov, M. A. *Izv. Acad. Nauk SSSR. Ser. Khim.* **1984**, 1166.
(83) Durif, A.; Averbuch-Pouchot, M. T.; Guitel, J. C. *Acta Crystallogr*. **1980**, *B36*, 680.
(84) Day, V. W.; Klemperer, W. G.; Maltbie, D. J. *J. Am. Chem. Soc.* **1987**, *109*, 2991.
(85) Day, V. W.; Klemperer, W. G.; Maltbie, D. J. *J. Am. Chem. Soc.* **1987**, *109*, 6030.
(86) Kato R.; Kobayashi, A.; Sasaki, Y. *Inorg. Chem.* **1982**, *21*, 240.
(87) Khan, M. I.; Zubieta, J.; Toscano, P. *Inorg. Chim. Acta* **1992**, *193*, 17.
(88) Harrison, A. T.; Howarth, O. W. *J. Chem. Soc., Dalton Trans.* **1985**, 1953.
(89) Hou, D.; Hagen, K. S.; Hill, C. L. *J. Chem. Soc. Chem. Commun.* **1993**, 426.
(90) Kempf, J. Y.; Rohmer, M. M.; Poblet, J. M.; Bo, C.; Bernard, M. *J. Am.Chem. Soc.* **1992**, *114*, 1136.
(91) Kidd, R. G. In *The multinuclear approach to NMR spectroscopy*; Lambert, J. B., Riddell, F. G., Eds.; NATO ASI Series; Reidel Publishing Company: 1983.
(92) Grieves R. A.; Mason, J. *Polyhedron* **1986**, *5*, 415.
(93) Sanchez, C.; Livage, J.; Launay, J. P.; Fornier, M. *J. Am. Chem. Soc*. **1983**, *105*, 6817.
(94) Kozik, M.; Hammer, C. F.; Baker, L. C. W. *J. Am. Chem. Soc.* **1986**, *108*, 2748.
(95) Rohmer, M.-M.; Benard, M. *Chem. Soc. Rev.* **2001**, *30*, 340.
(96) Cadot, E.; Béreau, V.; Marg, B.; Halut, S.; Secheresse, F. *Inorg. Chem.* **1996**, *35*, 3099.
(97) Kazansky, L. P.; Launay, J. P. *Chem. Phys. Lett.* **1977**, *51*, 242
(98) Piepgrass, K.; Pope, M. T. *J. Am. Chem. Soc.* **1987**, *109*, 1586.
(99) Santure, D. J.; McLaughlin, K. W.; Huffman, J. C.; Sattelberger, A. P. *Inorg. Chem.* **1983**, *22*, 1877.
(100) Dolbecq, A.; Cadot, E.; Eisner, D.; Secheresse, F. *Inorg. Chem*. **1999**, *38*, 4217.
(101) Barrows, J. N.; Jameson. J. B.; Pope, M. T. *J. Am. Chem. Soc.* **1981**, *107*, 1771.
(102) Ishikawa, E.; Yamase, T. *Bull. Chem. Soc. Jpn.* **2000**,*73*, 641.
(103) Pope, M. T. *Adv. Chem. Ser*. **1990**, *226*, 403.
(104) Kazansky, L. P.; Fedotov, M. A.; Potapova, I. V.; Spitsyn, V. I. *Dokl. Akad. Nauk. SSSR* **1979**, *244*, 372
(105) Barrows, J. N. Thesis, Georgetown University, 1982.
(106) Proust, A.; Thouvenot, R.; Roh, S.-G.; You, J.-K.; Gouzerh, P. *Inorg. Chem*. **1995**, *34*, 4106.
(107) Calzaferri G.; Rytz, R. *J. Phys. Chem.* **1995**, *99*, 12141.